

# ASVSim (AirSim for Surface Vehicles): A High-Fidelity Simulation Framework for Autonomous Surface Vehicle Research

Bavo Lesy<sup>a,\*</sup>, Siemen Herremans<sup>a,\*</sup>, Robin Kerstens<sup>b,c</sup>, Jan Steckel<sup>b,c</sup>, Walter Daems<sup>b,c</sup>, Siegfried Mercelis<sup>a</sup> and Ali Anwar<sup>a</sup>

<sup>a</sup>*IDLab, Faculty of Applied Engineering, University of Antwerp - imec, Sint-Pietersvliet 7, Antwerp, 2000, Belgium*

<sup>b</sup>*Cosys-Lab, Faculty of Applied Engineering, University of Antwerp, Groenenborgerlaan 171, Antwerp, 2020, Belgium*

<sup>c</sup>*Flanders Make Strategic Research Centre, Oude Diestersebaan 133, Lommel, 3920, Belgium*

## ARTICLE INFO

### Keywords:

Vessel Simulation  
Computer Vision  
Unmanned Surface Vehicles  
Open-Source  
Path Planning  
Deep Learning

## ABSTRACT

The transport industry has recently shown significant interest in unmanned surface vehicles (USVs), specifically for port and inland waterway transport. These systems can improve operational efficiency and safety, which is especially relevant in the European Union, where initiatives such as the Green Deal are driving a shift towards increased use of inland waterways. At the same time, a shortage of qualified personnel is accelerating the adoption of autonomous solutions. However, there is a notable lack of open-source, high-fidelity simulation frameworks and datasets for developing and evaluating such solutions. To address these challenges, we introduce AirSim For Surface Vehicles (ASVSim), an open-source simulation framework specifically designed for autonomous shipping research in inland and port environments. The framework combines simulated vessel dynamics with marine sensor simulation capabilities, including radar and camera systems and supports the generation of synthetic datasets for training computer vision models and reinforcement learning agents. Built upon Cosys-AirSim, ASVSim provides a comprehensive platform for developing autonomous navigation algorithms and generating synthetic datasets. The simulator supports research of both traditional control methods and deep learning-based approaches. Through limited experiments, we demonstrate the potential of the simulator in these research areas. ASVSim is provided as an open-source project under the MIT license, making autonomous navigation research accessible to a larger part of the ocean engineering community.

## 1. Introduction

There is a significant research effort concerning autonomous navigation systems for unmanned surface vehicles (USVs) (Gu et al., 2021; Pietrzykowski et al., 2022). However, developing and testing autonomous navigation systems in real-world environments is challenging due to high costs, safety risks, and the complex nature of maritime operations. For inland waterways, the complexity is further increased by narrow passages, locks, and dense traffic patterns and a frequent need to observe and avoid obstacles through the use of sensors. Infrastructure such as bridges, ports, and shore-based facilities may lead to sensor occlusion, creating blind spots that autonomous systems must account for. Additionally, varying wind and current conditions can significantly impact a vessel, requiring robust control strategies to maintain safe navigation. Because of these challenges, simulation has emerged as a crucial tool for developing and validating navigation algorithms, in a safe and cost-effective manner (Fossen, 2021; Zhang et al., 2024; Serigstad et al., 2018). For these purposes, it is important that the simulation closely represents the real world to reduce the effort needed to deploy simulated solutions on real vessels. However, a

current gap exists in the availability of shipping simulators for autonomy research, with most existing simulators either being designed for human operator training, being proprietary, or lacking the visual realism (or fidelity) needed for accurate camera and sensor simulation. More recently, there is an increasing interest in the potential of deep learning methods in a shipping context, such as obstacle detection (Jiang et al., 2024) or Reinforcement Learning (RL) for navigation (Herremans et al., 2023). RL has emerged as a promising approach for USVs, partly because of its ability to generalize across different vessel types and operating conditions (Lesy et al., 2024). However, the USV domain currently lacks accessible, high-fidelity simulation software that can accurately model vessel dynamics and generate realistic sensor data for development of autonomous systems that perceive their environment and navigate within it.

The main contribution of this paper is AirSim for Surface Vehicles (ASVSim)<sup>1</sup>, an open-source, high-fidelity simulator specifically designed for autonomous shipping research. ASVSim is tailored for Inland Waterway Transport (IWT), where the focus is more on the navigation of vessels through narrow passages and locks, and less on the dynamics of the vessel itself. The simulator currently provides 3-degree-of-freedom (3DoF) maneuvering dynamics, sensor simulations, and environmental conditions such as wind and currents. This enables researchers to develop, train, and test autonomous navigation algorithms in a configurable setting. As will be demonstrated throughout this work, ASVSim

\*Corresponding authors with equal contribution

 Bavo.Lesy@uantwerpen.be (B. Lesy);

Siemen.Herremans@uantwerpen.be (S. Herremans)

ORCID(S): 0009-0000-9395-9437 (B. Lesy); 0000-0001-7880-7144 (S. Herremans); 0000-0002-5127-4947 (R. Kerstens); 0000-0003-4489-466X (J. Steckel); 0000-0001-6717-744X (W. Daems); 0000-0001-9355-6566 (S. Mercelis); 0000-0002-5523-0634 (A. Anwar)

<sup>1</sup><https://github.com/BavoLesy/ASVSim>

**Table 1**  
Comparison of Marine Shipping Simulators (excluding underwater simulation)

Simulator	Open-source	High Fidelity	Primary Usage
SIMTECH ASHSS (Simtech, 2025)	×	✓	Autonomous navigation
Kongsberg K-Sim (Kongsberg, 2025)	×	✓	Maritime training
Nautis/Nautis Home (VSTEP Simulation, 2025)	×	✓	Maritime training
Wärtsilä R&D Simulator (Wärtsilä, 2025)	×	✓	Autonomous navigation
European Ship Simulator (Excalibur Games, 2016)	×	✓	Entertainment
uSimMarine (MOOS-IVP) (Benjamin et al., 2010)	✓	×	Autonomous navigation
Marine Systems Simulator (Fossen and Perez, 2004)	✓	×	Marine control systems
<b>ASVSim (ours)</b>	✓	✓	Autonomous navigation

allows for the creation of high-fidelity environments, essential for image-based sensor research. Because of this visual fidelity, ASVSim can be used to generate realistic synthetic datasets to train computer vision models. We demonstrate how the simulator can be used for training and validation of autonomy solutions, using examples such as dataset collection and waterway segmentation. Limited autonomous navigation tasks are demonstrated as example use-cases of the simulator, such as autonomous channel navigation and the training of a RL agent to navigate a vessel to a goal whilst avoiding obstacles.

The paper is structured as follows: in Section 2, we review related works in the field of shipping simulators. In Section 3 and 4, we provide an overview of the mathematical models used in ASVSim, describing vessel dynamics and radar simulation. In Section 5, we discuss the functionality and practical usage examples of ASVSim, based on the Cosys-AirSim (Jansen et al., 2023) framework, and demonstrate its ease of use through a Python and Matlab application programming interface (API). Furthermore, in Section 6, we present the results of our autonomy experiments, including computer vision and path planning tests. Finally, in Section 7, we provide a conclusion of our work and lay out future research directions.

## 2. Related Works

Mission simulation has long been an essential tool in the shipping industry, primarily for training and certification of maritime personnel. The evolution of these simulators has been driven by the need for increasingly realistic training environments that can prepare personnel for operating modern vessels. Industry-standard simulators such as Kongsberg K-Sim (Kongsberg, 2025) and Nautis (VSTEP Simulation, 2025) have become more and more present in maritime education, providing highly realistic environments with accurate vessel dynamics, environmental conditions, and operational scenarios. These commercial systems excel in their primary

use case: training maritime professionals in vessel handling, navigation, and emergency procedures across various vessel types and maritime conditions. These simulators offer realistic physics models and visualization of maritime scenarios with detailed rendering of weather conditions and accurate representations of navigational sensors and port infrastructure. Many include replicas of actual bridge equipment and instrumentation, closely mirroring real-world vessel operations. However, as these systems were designed primarily for human operators, they are not directly suitable for autonomy research. Additionally, these simulators are mostly closed-source and licenses can be expensive.

The limitations of these traditional training simulators have become apparent as the maritime industry increasingly embraces automation. While platforms such as SIMTECH (Simtech, 2025) and the Wärtsilä R&D Simulator (Wärtsilä, 2025) have begun incorporating features for autonomous vessel development, their proprietary nature and commercial focus create substantial barriers for academic research and open innovation. Entertainment-oriented simulators such as European Ship Simulator (Excalibur Games, 2016), though more accessible, lack the physical accuracy and sensor simulation capabilities essential for meaningful autonomy research. Several open-source maritime simulators have emerged to address the research gap in autonomous navigation, but each has significant limitations. MOOS-IVP (uSimMarine) (Benjamin et al., 2010), while providing a framework for autonomous vessel control, suffers from highly simplified dynamical modeling and is limited to a 2D visualization (via pMarineViewer) with minimal sensor simulation capabilities. Similarly, the Marine Systems Simulator (MSS) (Fossen and Perez, 2004), a Matlab/Simulink-based library for marine control systems development, offers elaborate physics models for various vessel types (ships, underwater vehicles, and unmanned underwater vehicles (UUVs)), but lacks integrated sensor simulation and comprehensive visualization capabilities. These

limitations significantly constrain the effectiveness of both simulators for developing and training autonomous maritime navigation systems. Simultaneously, the field of autonomous driving has benefited greatly from several open-source simulators with high visual fidelity such as CARLA (Dosovitskiy et al., 2017) and Cosys-AirSim (Jansen et al., 2023). These simulators excel at replicating real-world conditions through detailed graphics, precise physics models, and advanced sensor simulation. Such high-fidelity environments allow algorithms that were developed in simulation to transfer more effectively to real-world applications (Bu et al., 2021). Another benefit of this fidelity is the ability and flexibility to effectively recreate real-world scenarios. Simulators such as Stonefish (Grimaldi et al., 2025), OceanSim (Song et al., 2025) and NauSim (Ortiz-Toro et al., 2024), offer realistic underwater environments and diverse sensor capabilities for UUV development and testing. Additionally, UNavSim (Amer et al., 2023) and HoloOcean (Potokar et al., 2022) leverage the advanced capabilities of Unreal Engine (Epic Games, 2025) to further enhance simulation realism. However, these underwater-focused simulators are not suitable for inland shipping applications, as they primarily model underwater physics and UUV models and dynamics, in addition to the absence of dynamic obstacles and inland waterway environments.

Therefore, as summarized in Table 1, a critical gap exists in the inland shipping domain particularly for USVs: the lack of open-source, high-fidelity simulators that have the physical realism and the functionality required for inland autonomy research. Notably, this shortage is also present in high-quality datasets, with maritime data typically remaining limited, fragmented, or proprietary. For an overview of marine datasets, the reader is referred to Su et al. (2023) and Trinh et al. (2024). ASVSim addresses these challenges by providing an open-source simulator with high visual fidelity, serving the needs of autonomous navigation research, with particular attention to inland waterways and ports. Our platform prioritizes ease of use for deep learning and robotics research applications. Furthermore, the simulator can generate comprehensive, diverse datasets essential for training and validating autonomy solutions.

### 3. Dynamics Simulation

Since the main focus of this paper is inland waterway navigation, we opt for a 3DoF model, ignoring the heave, roll and pitch of the vessel. Specifically, we implement the 3DoF maneuvering model (see Figure 1), as presented by Fossen (2021). This model allows us to express the surge, sway and rotational velocity of the vessel, based on the force inputs and hydrodynamical constants that define the mass, damping and Coriolis and centripetal effects. Throughout this work, we will be using bold notation for vectors (e.g.  $\mathbf{x}$ ) and the dot notation for the derivatives of these vectors (e.g.  $\dot{\mathbf{x}}$ ). Additionally, matrices are denoted as capitalized bold symbols (e.g.  $\mathbf{M}$ ).

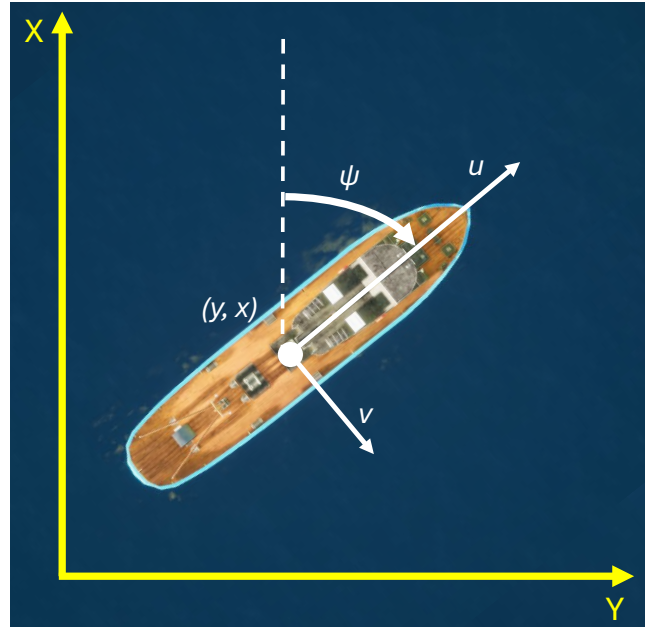


**Figure 1:** Visualization of the Fossen vessel model used in the simulation. The vessel has three degrees of freedom: surge, sway, and yaw.

#### 3.1. Kinematics

We describe the vessel's position with its positional coordinates and heading (in the Earth-fixed frame),  $\boldsymbol{\eta} = [x, y, \psi]$ . Secondly, we include the surge, sway and rotational velocity using  $\mathbf{v} = [u, v, r]$  in the body-fixed frame. The kinematics of these vectors are described by Eqn. (1).

$$\dot{\boldsymbol{\eta}} = \mathbf{R}_{rot}(\boldsymbol{\psi})\mathbf{v}$$

$$\mathbf{R}_{rot}(\boldsymbol{\psi}) = \begin{bmatrix} \cos(\boldsymbol{\psi}) & -\sin(\boldsymbol{\psi}) & 0 \\ \sin(\boldsymbol{\psi}) & \cos(\boldsymbol{\psi}) & 0 \\ 0 & 0 & 1 \end{bmatrix} \quad (1)$$

Furthermore, we allow for currents, which are described using a velocity vector  $\dot{\boldsymbol{\eta}}_c$  in the Earth-fixed frame. These can be translated to a local-frame current velocity vector  $\mathbf{v}_c$  via the (orthonormal) rotation matrix:

$$\mathbf{v}_c = \mathbf{R}_{rot}(\boldsymbol{\psi})^T \dot{\boldsymbol{\eta}}_c \quad (2)$$

$$\dot{\boldsymbol{\eta}}_c = [V_c \cdot \cos(\beta_c), V_c \cdot \sin(\beta_c), 0]^T \quad (3)$$

where  $V_c$  describes the velocity of the current (in  $m/s$ ) and  $\beta_c$  denotes the heading of the current in the Earth-fixed frame (in radians). Finally, the relative velocity vector  $\mathbf{v}_r$  is defined as the difference between the velocity of the ego vessel and the velocity of the current.

$$\mathbf{v}_r = \mathbf{v} - \mathbf{v}_c \quad (4)$$

#### 3.2. Dynamics

The dynamics are specified by five vessel-dependent  $3 \times 3$  matrices.  $\mathbf{M}_{RB}$  and  $\mathbf{M}_A$  are the rigid-body and

hydrodynamical mass matrices, defining the (added) mass of the vessel, the centers of gravity and the inertia around the yaw axis.  $C_{RB}(\mathbf{v})$  and  $C_A(\mathbf{v}_r)$  define the rigid body and hydrodynamical Coriolis (and centripetal) matrices. Finally,  $D(\mathbf{v}_r)$  represents the damping force acting on the vessel. Importantly,  $D(\mathbf{v}_r)$  is allowed to contain both linear and non-linear damping elements, such as  $u^2$ ,  $v^2$  and  $r^2$ . Eqn. 5 fully describes the dynamics, subject to an external control vector  $\tau$  and wind  $\tau_{wind}$ .

$$\begin{aligned} M_{RB}\dot{\mathbf{v}} + C_{RB}(\mathbf{v})\mathbf{v} + M_A\dot{\mathbf{v}}_r + \\ C_A(\mathbf{v}_r)\mathbf{v}_r + D(\mathbf{v}_r)\mathbf{v}_r = \tau + \tau_{wind} \end{aligned} \quad (5)$$

Many practical models ignore currents (i.e.  $\mathbf{v}_c = \mathbf{0}$ , where  $\mathbf{0}$  denotes a vector containing only zeros) (Zheng et al., 2014; Kristiansen et al., 2024), allowing a simplification of the dynamics by defining  $M = M_{RB} + M_A$  and  $C = C_{RB} + C_A$ . This simplified model (ignoring currents) is described in Eqn. 6.

$$M\dot{\mathbf{v}} + C(\mathbf{v})\mathbf{v} + D(\mathbf{v})\mathbf{v} = \tau + \tau_{wind} \quad (6)$$

However, as we believe that currents and wind are important factors to consider in autonomous navigation research. Therefore we include these currents, under the assumption that they are irrotational and (approximately) constant. These assumptions are commonly made when modeling vessels, since they allow for practical parameter estimation on real-world vessels. More details on this are provided in Section 3.4.

### 3.3. Control forces

The simulator allows to place an arbitrary amount of thrusters. Each of them is controlled by setting a thrust force  $F_i$  (in Newton) and the desired angle  $\theta_i$  (where  $i$  is the index of the thruster). Additionally, the position of each thruster can be configured using  $d_{x_i}$  and  $d_{y_i}$ , which represent the position of the thruster with regard to the center of gravity (COG). For example, a stern thruster can be created by placing it at the back of the vessel and limiting the minimal and maximal turning angle. Similarly, a bow thruster can be created by adding a thruster at the front of the vessel, and fixing its angle. We model the force of the thrusters on the vessel as follows:

$$\tau = \begin{bmatrix} \cos(\theta_1) & \dots & \cos(\theta_n) \\ \sin(\theta_1) & \dots & \sin(\theta_n) \\ d_{x_1} \sin(\theta_1) - d_{y_1} \cos(\theta_1) & \dots & d_{x_n} \sin(\theta_n) - d_{y_n} \cos(\theta_n) \end{bmatrix} \times \mathbf{f}, \quad (7)$$

where  $\mathbf{f} = [F_1, F_2, \dots, F_n]^T$  represents the vector containing all thruster forces. Similarly,  $\theta = [\theta_1, \theta_2, \dots, \theta_n]$  represents all thruster angles (in the local frame). The control input vector  $\tau$  contains the surge, sway and yaw components that are added to the system.

### 3.4. Currents

Eqn. 5 already includes the effect of currents, since it is parameterized on both  $\mathbf{v}$  and  $\mathbf{v}_r$ . However, separate parameter estimation for the rigid-body matrices (such as  $M_{RB}$ ) and the hydrodynamical matrices (such as  $M_A$ ) is impractical and uncommon in research, since it makes real-world parameter estimation impractical. Therefore, we follow the common assumption that currents are irrotational and constant over short time spans (Yoon and Rhee, 2003; Fossen, 2021; DeRensis, 2013). The irrotational property refers to the absence of a sway component in the current, as denoted in Eqn. 3. The constant property assumes that there is negligible acceleration of the current in the Earth-fixed frame, i.e.,  $\ddot{\eta}_c \approx \mathbf{0}$ . Under these ocean current assumptions, it is shown that, when we parametrize the  $C_{RB}$  matrix independent of surge and sway, the dynamics can be described as follows:

$$M\dot{\mathbf{v}}_r + C(\mathbf{v}_r)\mathbf{v}_r + D(\mathbf{v}_r)\mathbf{v}_r = \tau + \tau_{wind}, \quad (8)$$

where  $M$  and  $C$  are defined as in Section 3.2. This is a practical model, since it only requires parameter estimation for a singular mass, Coriolis and damping matrix. It is trivial to compute the absolute velocity from the relative velocity using Eqn. 4.

### 3.5. Implemented models

ASVSim allows to easily add specific damping and Coriolis models to compute  $C(\mathbf{v}_r)$  and  $D(\mathbf{v}_r)$ . Four models are already implemented and available in the simulator:

- MilliAmpere Ferry, an autonomous passenger ferry at Norwegian University of Science and Technology (NTNU) (Pedersen, 2019),
- Qiuxin No.5, a small research vessel at the Wuhan University of Technology (You et al., 2023),
- CyberShip II, a 1:70 scale replica of a supply ship, created for towing tank experiments (Skjetne et al., 2004).
- A full scale Mariner class cargo vessel (Chislett and Strom-Tejsen, 1965).

As an illustrative example of the simulated effect of currents on a vessel, we include Figure 2. This figure shows the recorded trajectories of the MilliAmpere ferry under no, low and moderate current velocities. As expected, currents with a higher velocity make the ferry move more from a straight path, and introduces torque on the vessel. Additionally, the current in the example decreases the speed of the vessel, as its impact angle has a component that is opposite to the thrust force direction.

## 4. Radar Simulation

Marine radio detection and ranging (radar) units are still dominant when it comes to localization, navigation,

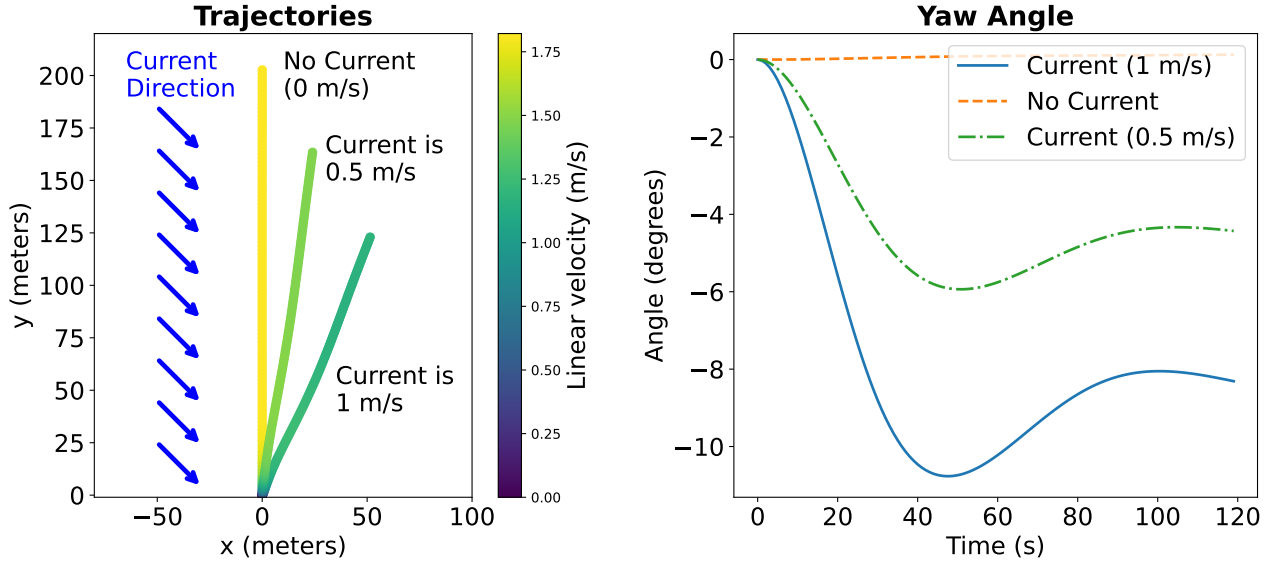


**Figure 2:** Sailing the MilliAmpere Ferry with thrust force at half ahead (250 Newton) with a straight thruster. Currents are simulated with an impact angle of  $135^\circ$  (top left). Left image: the recorded trajectories, starting from  $x = 0$ ,  $y = 0$ . Right image: the rotation around the yaw axis, induced by the current.

and collision avoidance in maritime environments. Although cameras and LiDAR systems are increasing in popularity, they cannot compete with the range that can be achieved with radar (Siciliano et al., 2008). Also, because of the familiarity between radar and the shipping industry, it makes sense to include a radar simulation in this simulation-based research. Cosys-Airsim (Jansen et al., 2023) has an accurate radar simulation based on ray-tracing techniques; however, this is based on a frequency modulated continuous wave (FMCW) radar unit originally introduced by Schouten et al. (2021), which is inherently different from the single-frequency pulse-echo systems commonly used in maritime and inland settings. For this reason, this research mimics a marine radar by using a modified version of the original AirSim (Shah et al., 2018) LiDAR implementation. The simulated LiDAR provides, at a predetermined frame rate that can be set similar to the rotation speed of the radar unit, a dense 3D point cloud of the surroundings covering a field-of-view of 360 degrees azimuth and a predetermined elevation. To mimic the performance of a maritime radar such as the Furuno DRS12A, as described in SAS (2025), the elevation was set to 20 degrees with a rotational angle of 36 RPM. This unit has a range of 69 NM. In this scenario, a maximum range of 5 km (2,7 NM) was chosen. This range is sufficient because the depth of measurement rarely exceeds this value due to occlusion by the buildings and infrastructure present in inland waterways. Furthermore, objects located outside of this 5 km range are deemed not relevant in this use-case and are in turn omitted to limit computing requirements. This simulated approach also offers the added benefit that the dense LiDAR point cloud contains the maximum number of reflections, which allows us to generate datasets with varying levels of sparsity, mimicking scenarios with reduced vision.

#### 4.1. Radar Detection Approximation and Visualization

Figure 3 illustrates the process used to mimic maritime radar data, starting from the original AirSim LiDAR sensor. An example LiDAR frame is shown in Figure 3a. Each simulated reflection obtained by the light pulses results in a set of cartesian coordinates. To mimic the typical visualization found on maritime radar displays, these LiDAR detection coordinates should be rasterized into an image, and should be convolved with the scanning radar point spread function (PSF) that can be expected at the locations of these points, as illustrated in Figure 3b. Figure 3c shows a close up of the same scene, highlighting the shape and orientation of the radar PSFs. The shape and orientation of this PSF is dependent on the properties of the radar, the range, and angle with respect to the location of the radar.

Starting from a set of input reflector points  $\mathbf{p}$ , obtained from the LiDAR simulation, the locations of the nearest and furthest points,  $\mathbf{p}_{\min}$  and  $\mathbf{p}_{\max}$ , with range  $\Delta\mathbf{p} = \mathbf{p}_{\max} - \mathbf{p}_{\min}$ , and image size  $G$ , the normalized point coordinates in the new image for each point  $\mathbf{p}'_i$  are:

$$\mathbf{p}'_i = \left\lceil \left( \frac{\mathbf{p}_i - \mathbf{p}_{\min}}{\Delta\mathbf{p}} \right) \cdot G \right\rceil \quad (9)$$

The direction vector  $\mathbf{d}_i$  from radar position  $\mathbf{p}_r$  to normalized point  $\mathbf{p}'_i$  is:

$$\mathbf{d}_i = \mathbf{p}'_i - \mathbf{p}_r \quad (10)$$

The range  $r_i$  is the Euclidean norm of  $\mathbf{d}_i$ :

$$r_i = \|\mathbf{d}_i\|_2 \quad (11)$$

As the radar PSF has its rotation with respect to the (centralized) location of the radar, the angle  $\theta_i$  can be found as:

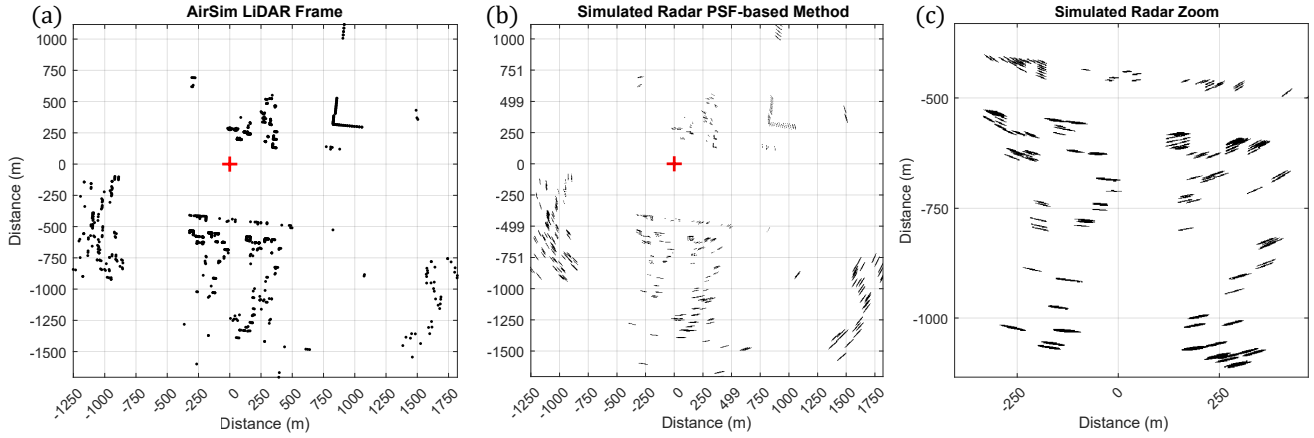


**Figure 3:** (a) The raw LiDAR point cloud obtained in the simulator. (b) The emulated radar data obtained using the PSF-based method (c) A subset of the center image, displaying the PSF varying over range and angle.

$$\theta_i = \arctan 2(d_{i,y}, d_{i,x}) \quad (12)$$

where  $d_{i,x}$  and  $d_{i,y}$  are the  $x$  and  $y$  components of  $\mathbf{d}_i$ , respectively. The basic shape of the radar PSF will be depicted as an ellipsoid (Richards et al., 2010), of which the semi-major axis  $a_i$  and semi-minor axis  $b_i$  are:

$$a_i = r_i \tan\left(\frac{\alpha}{2}\right) \frac{G}{\Delta p_x} \quad (13)$$

$$b_i = r_i \tan\left(\frac{\beta}{2}\right) \frac{G}{\Delta p_y} \quad (14)$$

where  $\alpha$  is the horizontal beam width of the radar unit in radians,  $\beta$  a scalar which is manually set to obtain the correct range resolution.  $\Delta p_x$  and  $\Delta p_y$  are the  $x$  and  $y$  components of  $\Delta \mathbf{p}$ , respectively. To fill-in the correct pixels in the new image, it is not possible to use a standard convolution method as our PSF varies for every different point in the image. Therefore, we use the ellipse indicator function  $E_i(x, y)$  is:

$$E_i(x, y) = \begin{cases} 1 & \text{if } \frac{x^2}{a_i^2} + \frac{y^2}{b_i^2} \leq 1 \\ 0 & \text{otherwise} \end{cases} \quad (15)$$

where:

$$x_c = x - p'_{i,x} \quad (16)$$

$$y_c = y - p'_{i,y} \quad (17)$$

$$x_r = x_c \cos(\theta_i) + y_c \sin(\theta_i) \quad (18)$$

$$y_r = -x_c \sin(\theta_i) + y_c \cos(\theta_i) \quad (19)$$

and  $p'_{i,x}$  and  $p'_{i,y}$  are the  $x$  and  $y$  components of  $\mathbf{p}'_i$ , respectively. The radar PSF  $P(x, y)$  is then the binary image that is obtained when taking the maximum of all ellipse indicator functions:

$$P(x, y) = \max_i E_i(x, y) \quad (20)$$

## 5. IDLab-ShippingSim

ASVSim is an extension of Cosys-AirSim (Jansen et al., 2023), a simulator primarily for autonomous cars, drones and robotics research. It is an extension of the original AirSim framework (Shah et al., 2018), initially developed by Microsoft Research to provide a realistic simulation environment for training and testing autonomous systems. Based on Unreal Engine 5 (UE5) (Epic Games, 2025), the simulator provides high-quality graphics and physics simulation. Additionally, Matlab and Python APIs are provided to allow simulation-based research without requiring knowledge of the simulator's internals. ASVSim also supports Procedural Generation (PCG) of environments (See Sec. 5.2). Because UE5 is used as a basis, we can leverage the blueprints system to easily change the simulation environments without writing code. With this visual scripting language, researchers can easily modify various aspects of the simulation, such as the objects in the waterway. Adjustments can include changing weather or time of day, altering the size, speed, orientation, and behavior of vessels, as well as changing camera perspectives to suit specific scenarios. Furthermore, it is straightforward to manipulate the environment to include new static and dynamic obstacles or change the layout. Researchers can also integrate custom 3-dimensional (3D) models or pre-existing assets from the Fab<sup>2</sup>, allowing for the creation of realistic and diverse environments tailored to research needs. In the first version of ASVSim, we have included three different basic example environments, a lake environment, a port environment, and a canal environment. These environments are shown in Figure 5. Lastly, ASVSim can run on most modern machines based on UE5 (Epic Games, 2025) recommended specifications: a quad-core CPU (2.5 GHz), 32 GB RAM, and an 8 GB graphics card. However, we have also successfully utilized the simulator on lower specification machines by adjusting the graphics settings appropriately.

<sup>2</sup><https://www.fab.com/>

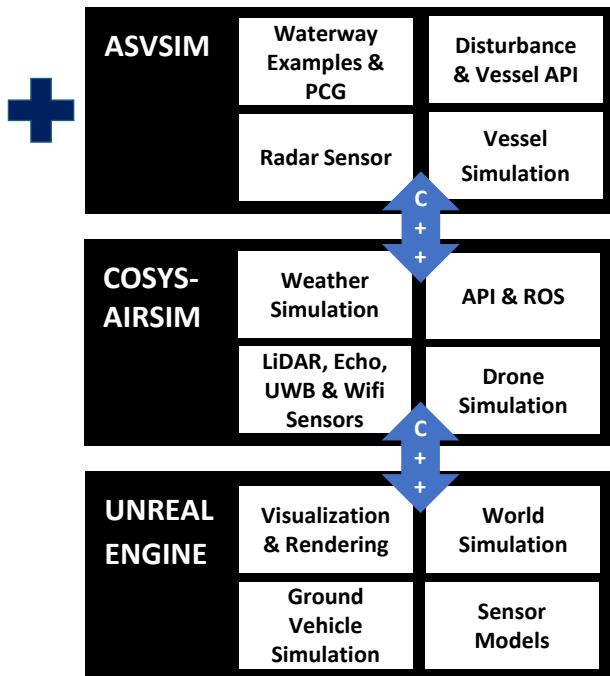


**Figure 4:** Overview of the ASVSim framework, showing the extensions and modifications to Cosys-AirSim. The simulator integrates specialized maritime dynamics models, radar simulation, and other features for autonomous vessel research.

ASVSim extends upon the work of Jansen et al. (2023) by adding vessel dynamics (see Sec. 3), including the modeling of disturbances such as currents and wind. We provide multiple vessel models, based on existing research vessels, together with inland waterway environments. Furthermore, we include radar simulation, as explained in Sec. 4. Finally, we extended the Python/Matlab API to include functionalities for controlling the vessel, changing disturbances, and retrieving sensor data (see Sec. 5.3). In Figure 4, an overview of the modifications and extensions to the Cosys-AirSim framework is shown. We also provide documentation<sup>3</sup> on the simulator and how to install, run and create your own projects. In Section 5.1, we highlight the annotated dataset generation functionality and in Section 5.3 we demonstrate how to control the simulator, both using the API.

### 5.1. Dataset Generation

Vision-based perception is essential for autonomous shipping systems in constrained inland waterway and port scenarios. Although computer vision techniques have been extensively applied in areas such as manufacturing and autonomous driving (Zhou et al., 2022; Kiran et al., 2021), progress in the maritime domain has been limited by the relative lack of annotated inland waterway vision datasets (Su et al., 2023; Trinh et al., 2024). Recent research (Bu et al., 2021) has shown that synthetic camera data generated from UE5 can significantly enhance the performance of object detection models on real-world data. To address this gap

<sup>3</sup><https://bavolesy.github.io/idlab-shippingsim-docs/>

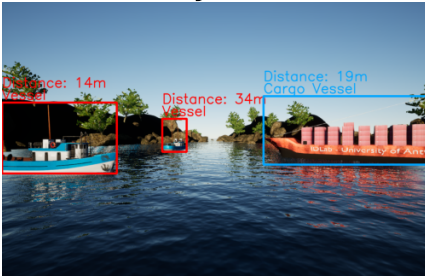


**Figure 5:** Overview of the example environments currently included in ASVSim.

in the ocean surface robotics community, we enable dataset generation for object detection, depth estimation, and image segmentation with their corresponding ground-truth labels.

Moreover, as ASVSim provides access to various sensors, such as LiDAR, radar, and depth camera, these datasets can also be used for sensor fusion tasks, which are increasingly important for advancing autonomy. For example, the depth camera captures precise distance measurements for each pixel in the image, which can be used to develop monocular depth estimation models (Spencer et al., 2023). These models are crucial for scenarios where only RGB cameras are available, enabling the estimation of distances to objects in the scene based solely on visual input (Lee, Wei-Yu and Jovanov, Ljubomir and Philips, Wilfried, 2021). Furthermore, combining depth estimation from RGB cameras with traditional radar systems allows for the detection of smaller objects that might be missed by radar alone due to low sparsity or quality (Ophoff et al., 2019). This enhanced optical precision is particularly important in IWT, where the presence of small obstacles, such as buoys, poses significant challenges for safe and reliable autonomous navigation. Furthermore, the simulator generates ground-truth labels for LiDAR point clouds, supporting dataset creation for 3D LiDAR-based object detection research, relevant for precise

### Camera: Object Detection



### Depth Image



### Segmentation Map

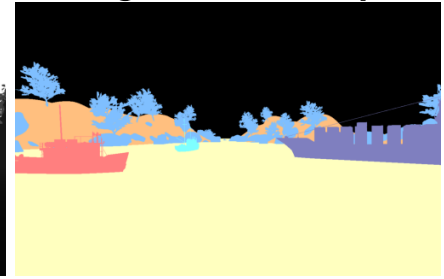


**Figure 6:** Example output from generated dataset. From left to right: bounding boxes generated automatically for vessels in the environment, depth camera measurements in grayscale (0 to 255m), segmentation map.

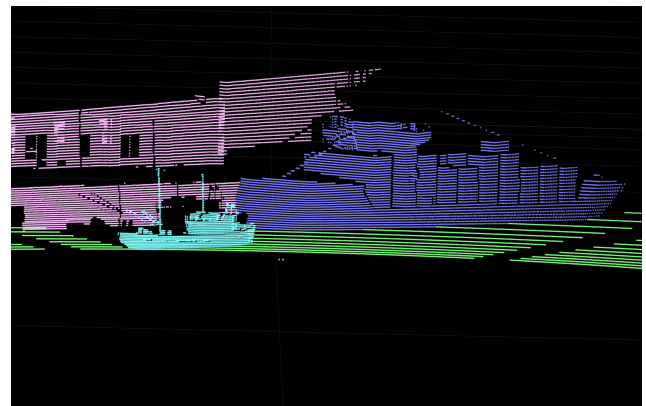
maneuvering such as docking or tugging. Figure 6 demonstrates the generated dataset, showing vessels detected by the semantic camera with depth camera measurements and automatically generated bounding boxes based on the semantic color mapping, along with the distance to these vessels. These images were collected using the `simGetImages()` command from the Python API. Additionally we generated a point cloud (see Figure 7) using the available LiDAR sensor and the Matlab API, via the command shown in Listing 1. This point cloud also automatically provides an instance segmentation ground truth. For more information on the LiDAR sensor, the reader is referred to Jansen et al. (2022).

## 5.2. Procedural Environment Generation

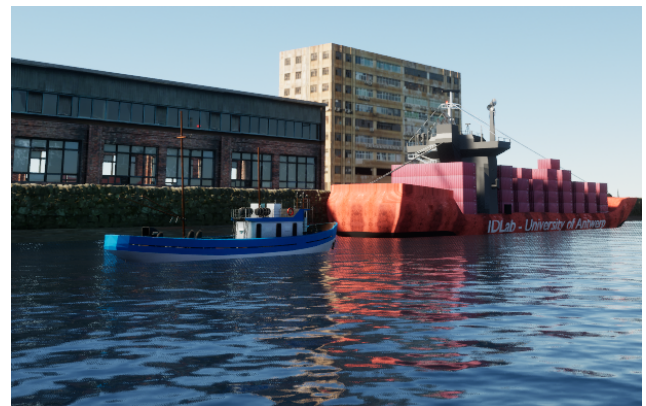
Recently, RL for autonomous navigation has gained significant interest. However, its success is often limited by the diversity of scenarios encountered during training. When trained in only a few environments, RL tends to struggle with generalizing to unseen situations. A common strategy to address this imitation is domain randomization (Tobin et al., 2017). By randomizing the environments and obstacles during training, RL may generalize better to unseen scenarios. Using the API, we can procedurally generate randomized port-like environments. When creating an environment, parameters such as the number of segments, random seed, width range, and the angle range between segments can be specified. In Figure 8, some examples of port-like environments can be seen. These can be generated at runtime, allowing for flexible RL training.

## 5.3. Controlling Vessels

Besides receiving the point cloud, Listing 1, provides a minimal example of how to control a vessel using the Matlab API. First, a connection to the running simulator is established. After the connection has been set up, measured state information can be received from a simulated Global Navigation Satellite System (GNSS) sensor. This includes information such as the current location, and velocities on the surge and sway axes. It is also possible to receive the acceleration vector of the vessel, using the available Inertial



(a)



(b)

**Figure 7:** (a) Generated point cloud, (b) corresponding camera image.

Measurement Unit (IMU) (allowing for Bayesian state estimation methods). More information about the ego vessel and its environment, such as wind speed and direction, the current time of day and the weather conditions are all available via the API. All sensor data, such as camera, LiDAR, radar and sonar sensors can also be read out.

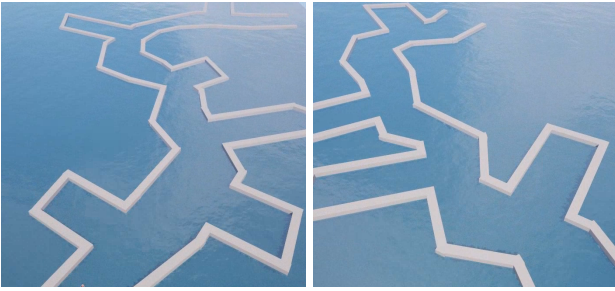


**Figure 8:** Example port-like waterways generated in ASVSim using the Python API. This environment can be used for training of RL agents for autonomous vessel navigation.

Listing 1: example on thrust control with a PID using the Matlab API

```

client = AirSimClient();
% Get LiDAR pointcloud p and
  semantic labels l
[p, l, ~, ~] = client.getLidarData(
  'Lidar1', true, '');
% Define PID with SimplePID(Kp, Ki,
  Kd)
pid = SimplePID(1.5, 1.0, 0.2);
desired_speed = 0.51 % in m/s
% Control loop
while true
  [gnssData, ~, ~] = client.
    getGpsData("Gps", '');
  velocity = gnssData.velocity;
  speed = sqrt(velocity(1).^2 +
    velocity(2).^2)
  thrust = pid.compute(
    desired_speed, speed)
  client.setVesselControls(thrust
    , 0.5, '');
  pause(0.1);
end

```

For an exhaustive summary of all API availability, we refer the reader to the documentation. With this sensor information, it is possible to manually control the vessel or use autonomous navigation algorithms to control all thrusters of the vessel. In the example, we set the thrust to 0.8 and the angle to 0.5 (both are normalized from 0 to 1, where an angle of 0.5 is equal to 0° and 0 and 1 represent the maximum angle of the thruster in both directions). This will make the vessel move forward in the surge direction with 80% of its maximum thrust. Additionally, non-controllable vessels can also be spawned, which are useful for testing the performance of navigational algorithms when other vessels are operating in the proximity of the ego vessel. Listing 1 furthermore displays a control loop that employs a proportional–integral–derivative (PID) controller to control the normalized thrust force on the (single-thruster) vessel. In this example case the PID is set to reach and hold a surge velocity of 1 knot.

## 6. Experiments

To further demonstrate the potential of ASVSim for autonomy research, we include three experiments. As we also include the source code for these experiments, they serve as a starting ground for future research. First, in Sec. 6.1, we evaluate an existing waterway segmentation model on synthetic data. Secondly, in Sec. 6.2, we perform two path planning experiments. The first experiment demonstrates a navigation approach, based on Dynamic Window Approach (DWA) (Fox et al., 1997), to navigate the MilliAmpere ferry (Brekke et al., 2022) in a restricted waterway. The second experiment trains an RL agent to navigate the ferry safely in a small-scale static obstacle avoidance setting.

### 6.1. Waterway Segmentation

In addition to the ability of collecting data (See Section 5.1), we investigate if an existing computer vision model (trained on real data) also works on the simulated camera images, without any retraining. For this, we perform a limited experiment, that employs the WaSR-T (Züst and Kristan, 2022) segmentation model in ASVSim. The WaSR-T model is specifically trained for waterway and obstacle segmentation in an inland context and hence closely aligns with the setting of this work. For the experiment, a trajectory is collected in a simulated inland waterway, using a camera mounted at the bow of the ego vessel (milliAmpere ferry). The recorded video (downsampled to 2 frames per second) is then segmented by the deep learning model.

Interestingly, WaSR-T succeeds in the segmentation task, even on simulated ASVSim data, as demonstrated by the results in Table 2 and further supported by the example in Figure 9. The model achieves a very high test score on segmenting the water class (all close to 0.99). Additionally, the model almost fully succeeds in differentiating between the sky and obstacles, however, the model sometimes does not capture all minor details, such as strips of air that are visible through windows of buildings. This good performance of WaSR-T on the synthetic data demonstrates the potential of ASVSim for preliminary validation of computer vision models during research, and suggests that the simulator could indeed be used for efficient pre-training of deep learning models. However, we leave a more elaborate investigation of these aspects for future work, as results are expected to be highly dependent on how visually realistic the UE5 environments are made.

### 6.2. Path Planning

Within the field of autonomous navigation, path planning is the process of determining a feasible path for an object, in this case a vessel, to navigate from a starting point to a goal location. The general problem of path planning can be divided into two main categories: global and local path planning. Global path planning algorithms find a static path from the starting position to a goal, whilst local path planning algorithms aim to navigate safely between two points on that global path. The determined path must avoid collisions with obstacles. For inland shipping, this becomes

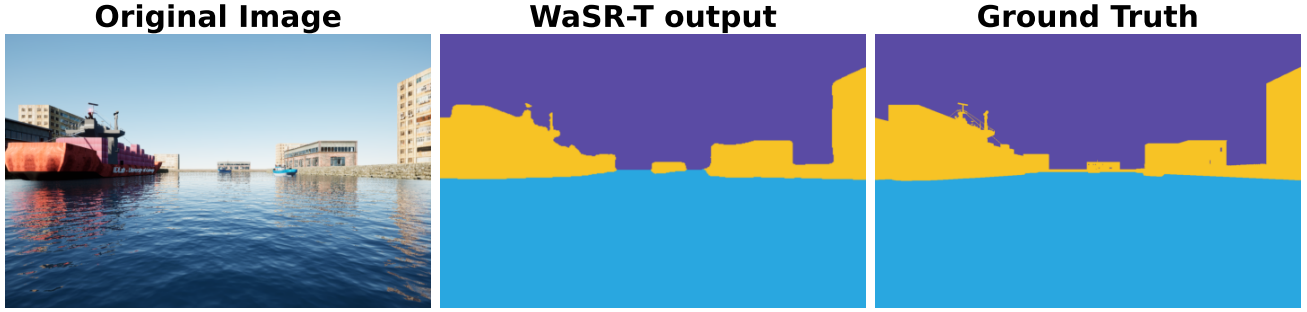


**Figure 9:** A representative example output of the WaSR-T model (Žust and Kristan, 2022). From left to right: the original simulated image, the WaSR-T output, and the ground-truth segmentation map. Blue denotes the waterway, purple denotes sky, yellow denotes all obstacles.

Metric	Water	Air	Other
IoU	0.9916	0.9859	0.9418
Precision	0.9971	0.9973	0.9806
Recall	0.9945	0.9885	0.9598

**Table 2**

Average test metrics of the WaSR-T model (Žust and Kristan, 2022) during a simulated test trajectory. Intersection over Union (IoU), Precision, and Recall for Water, Air, and Obstacle classes are shown. Precision and recall are calculated by considering the segmentation task as a pixel-wise classification problem.

increasingly complex as the vessel must take into account various constraints, such as fuel consumption or regulatory and physical constraints. ASVSim has functionality for researchers to implement and test both traditional navigation methods and RL algorithms for path planning. We demonstrate this functionality in Sections 6.2.1 and 6.2.2

### 6.2.1. Autonomous Navigation with DWA

As ASVSim is focused on IWT navigation, we consider a local path planning experiment, assuming that a global path is provided. For local path planning, the DWA (Fox et al., 1997) algorithm has been used in a number of applications for navigation and collision avoidance for USVs (Serigstad et al., 2018; Kim et al., 2021). The advantage of DWA over other common methods such as  $A^*$  (Hart et al., 1968) or  $RTT^*$  (Karaman and Frazzoli, 2011) is its ability to ensure that generated paths are dynamically feasible. The approach works by creating a window of possible linear and angular velocities whilst taking into account the current dynamics of the vessel. All admissible velocity pairs are then evaluated with a predefined cost function over a trajectory with a finite horizon. To calculate admissible trajectories, the dynamics model of the vessel is used. The cost function that was used in the experiment is displayed in Eqn. 21. To implement DWA, we opted for the PythonRobotics library (Sakai et al.,

2018). We integrated the algorithm with the simulator and tested it on a channel-navigation scenario with a number of obstacles. A radar (see Sec. 4) was used to detect the edges of the channel and other obstacles (such as moored vessels). The radar scan is then used to create an obstacle map, which in turn is used to calculate the cost function for each trajectory in the dynamic window. The trajectory with the lowest cost is then chosen and executed. The cost function is defined as follows:

$$C_{total} = C_{speed} + C_{obstacle} + C_{goal} \quad (21)$$

where  $C_{speed}$  is the cost related to how fast the vessel travels,  $C_{obstacle}$  is the cost of how close the vessel is to obstacles, and  $C_{goal}$  is the cost of how close the vessel is to the goal. These costs are calculated as follows:

$$C_{goal} = G_{goal} \cdot \arctan \left( \frac{\sin(\theta_{goal} - \theta_{vessel})}{\cos(\theta_{goal} - \theta_{vessel})} \right)$$

$$C_{obstacle} = G_{obstacle} \cdot \begin{cases} \frac{1}{d_{min}} & \text{if } d_{min} > d_{threshold} \\ +\infty & \text{otherwise} \end{cases} \quad (22)$$

$$C_{speed} = G_{speed} \cdot (v_{max} - v_{vessel})$$

with  $G_{goal}$ ,  $G_{obstacle}$ , and  $G_{speed}$  being constants to weigh the importance of each cost.  $d_{min}$  represents the minimum distance to obstacles along the trajectory, while  $d_{threshold}$  denotes the vessel's dimensions. A collision is assumed when  $d_{min} < d_{threshold}$ , and the cost is set to  $+\infty$ .  $x_{goal}$  and  $y_{goal}$  are the coordinates of the goal,  $x_{vessel}$  and  $y_{vessel}$  are the position coordinates of the vessel,  $\theta_{vessel}$  is the orientation of the vessel and  $v_{max}$  is the maximum velocity of the vessel. After manual tuning of the cost function and configuring the parameters, the vessel navigated the path without collisions. This scenario is visualized, along with the corresponding radar detection, in Figure 10. Although DWA navigates the channel successfully, it must be stated that the high computational cost is a significant downside of the methodology. This downside can be important for

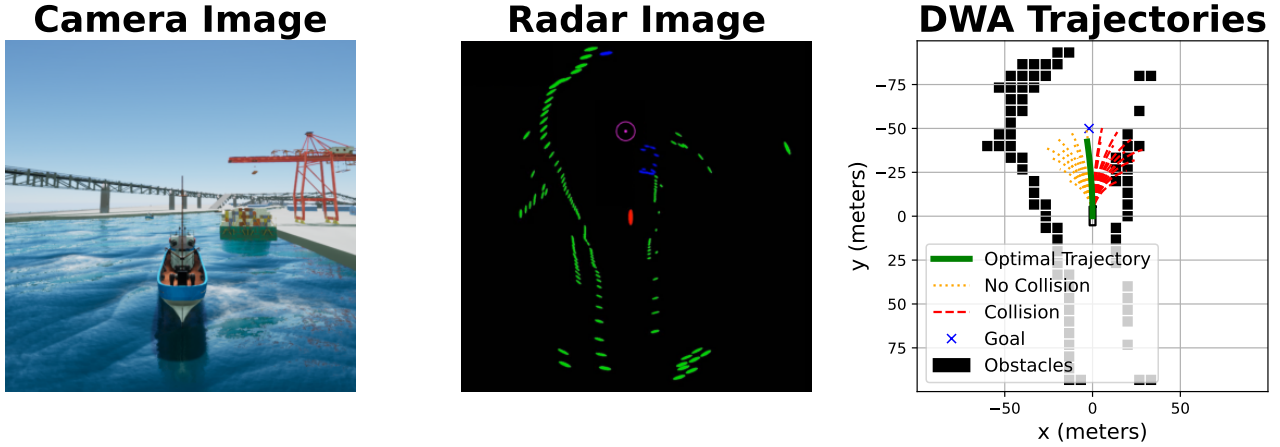


**Figure 10:** Overview of the path planning experiment with DWA to navigate a vessel through a channel. From left to right: Camera image, Radar image (with goal as purple circle), and simulated DWA trajectories.

long-horizon problems such as vessel navigation, especially in busy IWT scenarios, where the situation can change significantly over a short period of time.

### 6.2.2. Reinforcement Learning

As mentioned in 6.2.1, a key limitation of DWA is its computational complexity, which scales poorly with the resolution of possible trajectories and trajectory length, with a computation time of more than 3 seconds for every timestep in our experiments. Another significant disadvantage of traditional control methods such as DWA is the need to manually adjust various parameters, in addition to the cost function, such as window size, time horizon, and velocity resolutions. To address these limitations, recent research has shown promising results using RL for path planning in autonomous shipping (Zhang et al., 2024; Lesy et al., 2024). In this section, we demonstrate how ASVSim can be used to train RL agents for autonomous navigation in shipping applications. RL (Sutton et al., 1998) is used to solve sequential decision-making problems where an agent learns an optimal strategy through interaction with an environment. These problems are modeled as Markov Decision Processes (MDPs). An MDP can be defined as a tuple  $(S, A, P, R, \gamma)$ , where  $S$  is the set of states,  $A$  is the set of actions,  $P$  is the transition probability function, which defines the probability of transitioning from one state to another given an action,  $R$  is the reward function, and  $\gamma$  is the discount factor, which balances immediate rewards with future returns. The agent's goal is to learn an optimal policy that maps states to actions to maximize the cumulative reward across the horizon  $H$ . The definition of the optimal policy can be seen in Eqn. 23.

$$\pi^* = \arg \max_{\pi} \left[ \mathbb{E}_{a \sim \pi} \left( \sum_{t=0}^H \gamma^t R(s_t, a_t) \right) \right] \quad (23)$$

Through continuous interaction with the environment, the agent learns an optimal policy by exploring different actions and updating its strategy based on received rewards.

This continuous interaction can be problematic for existing systems, since learning policies on a real vessel can be time-consuming, costly and dangerous. Furthermore, for autonomous shipping solutions to achieve commercial viability, they must demonstrate robust generalization across different vessels and maritime environments. Our previous research (Lesy et al., 2024) has demonstrated that RL-based approaches maintain strong performance across vessels with varying physical properties, such as mass, without requiring retraining or extensive manual recalibration. This represents a significant advantage over traditional control methods, which typically require substantial domain expertise and manual tuning for each new vessel configuration. The success of RL algorithms heavily depends on training with diverse, representative data. ASVSim addresses this need by enabling the creation of varied training scenarios with dynamic obstacle configurations, different weather and water conditions, and various port and waterway layouts. This rich simulation environment allows for training of agents across a wide range of IWT scenarios. As a proof of concept, we trained an agent to autonomously navigate a vessel in an example environment with a fixed goal and fixed static obstacles. We included this experiment in the code release, which can be used as a starting point for research towards RL agents in ASVSim. In our test environment, the goal position, starting position and obstacles remain fixed between scenarios or episodes. However, the same approach can be extended to more complex environments, for example with procedurally generated elements.

In our experiment, at every timestep, the agent receives an observation containing the vessel state and radar data. This observation is then passed into the agent, which outputs an action, which is then executed in the environment. The agent then receives another observation and a reward based on the action and the state of the environment. This process is repeated until the agent reaches the goal or collides with an obstacle. When an episode ends, the vessel is placed back at the starting position. In this example, the control frequency

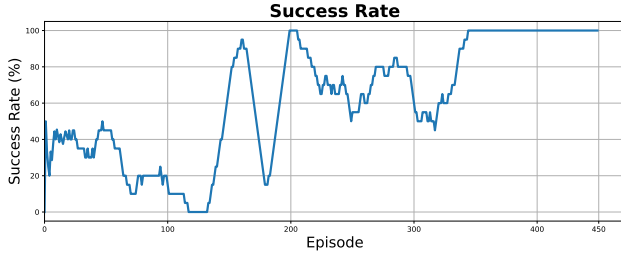


**Figure 11:** Success rate of the RL agent during. Reaching the goal is classified as a success. After around 350 episodes, the agent has learned a policy which successfully reaches the goal 100% of the time

is set to 1 Hz, which means that a step in the environment is equivalent to 1 second in real time. The observation space for the RL agent consists of the following components; The distance between the vessel and the goal is defined in  $d_{goal}$ ,  $\theta$  is the heading of the vessel,  $\mathbf{v}$  is the velocity of the vessel and  $\dot{\mathbf{v}}$  is the acceleration of the vessel (in the body-fixed frame). The previous actions are represented by  $a_{t-1}$  and  $\mathbf{d}_{obstacles}$  represents the distances towards the obstacles as detected by the radar sensor (4). The observation at timestep  $t$  can be seen in Eqn. 24.

$$\mathbf{obs}_t = [d_{goal}, \theta, \mathbf{v}, \dot{\mathbf{v}}, a_{t-1}, \mathbf{d}_{obstacles}] \quad (24)$$

The agent has a continuous 2-dimensional action space controlling the vessel's thrust force (0 to 1) and thruster angle (0.4 to 0.6), with the same controls as in Sec. 5.3. In this scenario, the thruster angle is constrained to limit the number of ineffective actions in the action space. The reward function is a weighted sum of the distance to the goal, the direction of the vessel, the heading of the vessel and the episode end. The full reward function can be seen in Eqn. 25. A positive  $\Delta d_{goal}$  indicates that the vessel is moving closer to the goal, while a negative value indicates it is moving away. This term is incorporated into the reward function to encourage the agent to minimize the distance to the goal. At the end of an episode, the agent receives a reward of 500 if the goal is reached, and -500 otherwise. Whilst the reward function could be improved upon to include information such as the distance to the obstacles or action consistency, in this example we opted for a simple reward function for clarity.

$$\begin{aligned} R_{distance} &= -d_{goal} \\ R_{direction} &= d_{goal}^{t-1} - d_{goal}^t \\ R_{heading} &= -\Delta\theta_{goal} \\ R_{end} &= \begin{cases} 500 & \text{if goal reached} \\ -500 & \text{otherwise} \end{cases} \end{aligned} \quad (25)$$

Reward function:

$$R(s_t, a_t) = G_1 \cdot R_{distance} + G_2 \cdot R_{direction}$$

$$+ G_3 \cdot R_{heading} + R_{end} \quad (26)$$

The algorithm used for the RL agent was the Stable Baselines (Raffin et al., 2021) implementation of the Soft Actor-Critic algorithm (Haarnoja et al., 2018). As seen on Figure 11, after training for 450 episodes, the agent was able to navigate the vessel to the goal while avoiding all obstacles successfully 100% of the time. The algorithm was trained for 8 hours on a system with an Intel i7-1260P, 32GB of system memory and an NVIDIA T550 graphics card, responsible for simulation and RL training. This demonstrates that the simulator can effectively run without extensive hardware requirements.

## 7. Discussion

### 7.1. Future Work

ASVSim provides a solid foundation for autonomous shipping research and opens up numerous research opportunities. Examples include the evaluation of reinforcement learning algorithms under varying environmental conditions, development and testing of perception algorithms for obstacle detection and classification, and researching of multi-vessel coordination strategies in congested waterways. Nevertheless, there are several directions for future development that would further enhance the simulator's capabilities. Our research group has recently conducted experimental trials with an USV equipped with various sensors such as a depth camera, LiDAR, and IMU. A key direction for future work involves performing system identification, similar to the work presented in (Pedersen, 2019), on this USV to precisely determine the parameters corresponding to its dynamics model. This will enable us to create a digital model of our USV in ASVSim and to simulate its dynamics. Such precise modeling may allow for the development of navigation algorithms and training of RL agents in simulation that can be effectively transferred to the physical vessel with minimal performance degradation. Furthermore, we plan to create more detailed and expansive inland waterway environments to generate realistic datasets and to train RL agents to autonomously navigate in these environments. We also aim to add more vessel models for IWT applications, including 6-degree-of-freedom (6DoF) models. Lastly, another possible direction for future work is to develop more sensor models, including multi-beam echosounders and radar-based positioning systems, such as radar beacons (RACONs). By releasing our work in an open-source manner, we invite the broader research community to collaborate, contribute, and extend its capabilities. Through collaboration, we hope to accelerate innovation in inland autonomous navigation research.

### 7.2. Conclusion

In this paper, we presented ASVSim, an open-source simulation framework specifically designed for autonomous shipping research. This simulator addresses a current gap in the research domain, where no open-source simulators with high visual fidelity are available. By combining vessel

dynamics models with relevant sensor simulations, we provide an extensive platform for developing and evaluating autonomous technologies for inland shipping applications. The experiments conducted on waterway segmentation and path planning demonstrate ASVSim's effectiveness in generating realistic sensor data and modeling vessel dynamics in inland waterway environments.

## 8. Declaration of generative AI and AI-assisted technologies in the writing process.

During the preparation of this work the authors used Claude 3.7 Sonnet in order to proofread and improve readability and language of the work. After using this tool/service, the authors reviewed and edited the content as needed and take full responsibility for the content of the published article.

## 9. Acknowledgments

This work was conducted within the Horizon 2020 PIONEERS project, funded by the European Commission under agreement No. 101037564. This work was supported by the Research Foundation Flanders (FWO) under Grant Number 1SHAI24N.

## CRedit authorship contribution statement

**Bavo Lesy:** Conceptualization, Investigation, Software, Writing - original draft. **Siemen Herremans:** Conceptualization, Investigation, Software, Writing - original draft. **Robin Kerstens:** Methodology, Software, Writing - original draft. **Jan Steckel:** Funding acquisition, Supervision. **Walter Daems:** Funding acquisition, Supervision. **Siegfried Mercelis:** Funding acquisition, Supervision. **Ali Anwar:** Writing - review & editing, Funding acquisition, Supervision.

## References

Amer, A., Álvarez-Tuñón, O., Uğurlu, H.İ., Le Fevre Sejersen, J., Brodskiy, Y., Kayacan, E., 2023. Unav-sim: A visually realistic underwater robotics simulator and synthetic data-generation framework, in: 2023 21st International Conference on Advanced Robotics (ICAR), pp. 570–576. doi:10.1109/ICAR58858.2023.10406819.

Benjamin, M.R., Schmidt, H., Newman, P.M., Leonard, J.J., 2010. Nested autonomy for unmanned marine vehicles with moos-ivp. *Journal of Field Robotics* 27, 834–875. doi:10.1002/rob.20370.

Brekke, E., Eide, E., Eriksen, B.O., Wilthil, E., Breivik, M., Skjellaug, E., Helgesen, O., Lekkas, A., Martinsen, A.B., Thyri, E., Torben, T., Veitch, E., Alsos, O., Johansen, T., 2022. milliamper: An autonomous ferry prototype. *Journal of Physics: Conference Series* 2311, 012029. doi:10.1088/1742-6596/2311/1/012029.

Bu, T., Zhang, X., Mertz, C., Dolan, J.M., 2021. Carla simulated data for rare road object detection, in: 2021 IEEE International Intelligent Transportation Systems Conference (ITSC), IEEE. pp. 2794–2801.

Chislett, M., Strom-Tejsen, J., 1965. Planar motion mechanism tests and full-scale steering and manoeuvring predictions for a mariner class vessel. *International Shipbuilding Progress* 12, 201–224.

DeRensis, T.P., 2013. A robust linear dynamic positioning controller for a marine surface vehicle. Ph.D. thesis. URL: <https://www.proquest.com/dissertations-theses/robust-linear-dynamic-positioning-controller/docview/1443861503/se-2>. copyright - Database copyright ProQuest LLC; ProQuest does not claim copyright in the individual underlying works; Last updated - 2023-03-04.

Dosovitskiy, A., Ros, G., Codevilla, F., Lopez, A., Koltun, V., 2017. Carla: An open urban driving simulator, in: *Conference on robot learning*, PMLR. pp. 1–16.

Epic Games, 2025. Unreal engine. <https://www.unrealengine.com/> (accessed 21 March 2025).

Excalibur Games, 2016. European ship simulator. [https://store.steampowered.com/app/299250/European\\_Ship\\_Simulator/](https://store.steampowered.com/app/299250/European_Ship_Simulator/) (accessed 11 April 2025).

Fossen, T., 2021. Handbook of Marine Craft Hydrodynamics and Motion Control. doi:10.1002/9781119994138.

Fossen, T.I., Perez, T., 2004. Marine Systems Simulator (MSS). <https://github.com/cybergalactic/MSS> (accessed 21 March 2025).

Fox, D., Burgard, W., Thrun, S., 1997. The dynamic window approach to collision avoidance. *IEEE Robotics & Automation Magazine* 4, 23–33.

Grimaldi, M., Cieslak, P., Ochoa, E., Bharti, V., Rajani, H., Carlucho, I., Koskinopoulou, M., Petillot, Y.R., Gracias, N., 2025. Stonefish: Supporting machine learning research in marine robotics. arXiv preprint arXiv:2502.11887.

Gu, Y., Goez, J.C., Guajardo, M., Wallace, S.W., 2021. Autonomous vessels: state of the art and potential opportunities in logistics. *International Transactions in Operational Research* 28, 1706–1739.

Haarhoja, T., Zhou, A., Abbeel, P., Levine, S., 2018. Soft actor-critic: Off-policy maximum entropy deep reinforcement learning with a stochastic actor, in: *International conference on machine learning*, Pmlr. pp. 1861–1870.

Hart, P.E., Nilsson, N.J., Raphael, B., 1968. A formal basis for the heuristic determination of minimum cost paths. *IEEE transactions on Systems Science and Cybernetics* 4, 100–107.

Herremans, S., Anwar, A., Troch, A., Ravijts, I., Vangeneugden, M., Mercelis, S., Hellinckx, P., 2023. Autonomous port navigation with ranging sensors using model-based reinforcement learning, in: *Volume 5: Ocean Engineering*, American Society of Mechanical Engineers. doi:10.1115/omae2023-104455.

Jansen, W., Huebel, N., Steckel, J., 2022. Physical lidar simulation in real-time engine, in: *2022 IEEE Sensors*, IEEE. pp. 1–4.

Jansen, W., Verreycken, E., Schenck, A., Blanquart, J.E., Verhulst, C., Huebel, N., Steckel, J., 2023. Cosys-airsim: A real-time simulation framework expanded for complex industrial applications, in: *2023 Annual Modeling and Simulation Conference (ANNSIM)*, pp. 37–48.

Jiang, Z., Su, L., Sun, Y., 2024. Yolov7-ship: A lightweight algorithm for ship object detection in complex marine environments. *Journal of Marine Science and Engineering* 12. doi:10.3390/jmse12010190.

Karaman, S., Frazzoli, E., 2011. Sampling-based algorithms for optimal motion planning. *The international journal of robotics research* 30, 846–894.

Kim, H.G., Yun, S.J., Choi, Y.H., Ryu, J.K., Suh, J.H., 2021. Collision avoidance algorithm based on colregs for unmanned surface vehicle. *Journal of Marine Science and Engineering* 9, 863.

Kiran, B.R., Sobh, I., Talpaert, V., Mannion, P., Al Sallab, A.A., Yogamani, S., Pérez, P., 2021. Deep reinforcement learning for autonomous driving: A survey. *IEEE transactions on intelligent transportation systems* 23, 4909–4926.

Kongsberg, 2025. K-sim navigation. <https://marsim.kongsbergdigital.com/products/k-sim/k-sim-navigation/> (accessed 21 March 2025).

Kristiansen, R., Ørke, H.L., Gravdahl, J.T., 2024. Modelling and simulation of interaction forces in tugboat-assisted docking of large marine vessels. *Simulation Modelling Practice and Theory* 130, 102866.

Lee, Wei-Yu and Jovanov, Ljubomir and Philips, Wilfried, 2021. Semantic-guided radar-vision fusion for depth estimation and object detection, in: *BMVC, the 32nd British Machine Vision Conference, Proceedings*, p. 13.

- Lesy, B., Anwar, A., Mercelis, S., 2024. Evaluating robustness of reinforcement learning algorithms for autonomous shipping. arXiv preprint arXiv:2411.04915 doi:10.48550/arXiv.2411.04915.
- Ophoff, T., Van Beeck, K., Goedemé, T., 2019. Exploring rgb+ depth fusion for real-time object detection. *Sensors* 19, 866.
- Ortiz-Toro, C.A., Cerrada-Collado, C., Moreno-Salinas, D., Chaos-García, D., García-Suárez, K.L., Otero-Roth, P., Vidal-Pérez, J.M., Luque-Nieto, M.A., Vázquez, A.I., Fraile-Ardanuy, J.J., Negro-Valdecantos, V., Jiménez-Yguacel, E., Aranda-Almansa, J., Zazo-Bello, S., Zufiria, P.J., Magdalena-Layos, L., Parras-Moral, J., Gutiérrez, A., 2024. Exploring uuv development with nausim: An open-source simulation platform, in: 2024 Global Conference on Wireless and Optical Technologies (GCWOT), pp. 1–7. doi:10.1109/GCWOT63882.2024.10805602.
- Pedersen, A.A., 2019. Optimization based system identification for the milliAmpere ferry. Master's thesis. NTNU.
- Pietrzykowski, Z., Wolejsza, P., Nozdrykowski, L., Borkowski, P., Banas, P., Magaj, J., Chomski, J., Maka, M., Mielniczuk, S., Panka, A., et al., 2022. The autonomous navigation system of a sea-going vessel. *Ocean Engineering* 261, 112104.
- Potokar, E., Ashford, S., Kaess, M., Mangelson, J.G., 2022. Holocean: An underwater robotics simulator, in: 2022 International Conference on Robotics and Automation (ICRA), IEEE. pp. 3040–3046.
- Raffin, A., Hill, A., Gleave, A., Kanervisto, A., Ernestus, M., Dormann, N., 2021. Stable-baselines3: Reliable reinforcement learning implementations. *Journal of Machine Learning Research* 22, 1–8. URL: <http://jmlr.org/papers/v22/20-1364.html>.
- Richards, M.A., Scheer, J., Holm, W.A., Melvin, W.L., 2010. Principles of modern radar.
- Sakai, A., Ingram, D., Dinius, J., Chawla, K., Raffin, A., Paques, A., 2018. Pythonrobotics: a python code collection of robotics algorithms. arXiv preprint arXiv:1808.10703 doi:10.48550/arXiv.1808.10703.
- SAS, F.F., 2025. Drs12a product page. <https://www.furuno.fr/en/lang--en--art--DRS12A-NXT--DRS12A-NXT.html> (accessed 11 March 2025).
- Schouten, G., Jansen, W., Steckel, J., 2021. Simulation of pulse-echo radar for vehicle control and slam. *Sensors* 21, 523.
- Serigstad, E., Eriksen, B.O.H., Breivik, M., 2018. Hybrid collision avoidance for autonomous surface vehicles. *IFAC-PapersOnLine* 51, 1–7. URL: <https://www.sciencedirect.com/science/article/pii/S2405896318321499>, doi:<https://doi.org/10.1016/j.ifacol.2018.09.460>. 11th IFAC Conference on Control Applications in Marine Systems, Robotics, and Vehicles CAMS 2018.
- Shah, S., Dey, D., Lovett, C., Kapoor, A., 2018. Airsim: High-fidelity visual and physical simulation for autonomous vehicles, in: Hutter, M., Siegwart, R. (Eds.), *Field and Service Robotics*, Springer International Publishing, Cham. pp. 621–635.
- Siciliano, B., Khatib, O., Kröger, T., 2008. *Springer handbook of robotics*, volume 200. Springer.
- Simtech, 2025. Ashss simulator. <https://www.simtech.spb.ru/en/ashss> (accessed 21 March 2025).
- Skjetne, R., Øyvind Smogeli, Fossen, T.I., 2004. Modeling, identification, and adaptive maneuvering of cybership ii: A complete design with experiments. *IFAC Proceedings Volumes* 37, 203–208. URL: <https://www.sciencedirect.com/science/article/pii/S1474667017317329>, doi:[https://doi.org/10.1016/S1474-6670\(17\)31732-9](https://doi.org/10.1016/S1474-6670(17)31732-9). iFAC Conference on Computer Applications in Marine Systems - CAMS 2004, Ancona, Italy, 7-9 July 2004.
- Song, J., Ma, H., Bagoren, O., Sethuraman, A.V., Zhang, Y., Skinner, K.A., 2025. Oceansim: A gpu-accelerated underwater robot perception simulation framework. arXiv preprint arXiv:2503.01074.
- Spencer, J., Qian, C.S., Trescakova, M., Russell, C., Hadfield, S., Graf, E.W., Adams, W.J., Schofield, A.J., Elder, J., Bowden, R., Anwar, A., Chen, H., Chen, X., Cheng, K., Dai, Y., Hoa, H.T., Hossain, S., Huang, J., Jing, M., Li, B., Li, C., Li, B., Liu, Z., Mattoccia, S., Mercelis, S., Nam, M., Poggi, M., Qi, X., Ren, J., Tang, Y., Tosi, F., Trinh, L., Uddin, S.M.N., Umair, K.M., Wang, K., Wang, Y., Wang, Y., Xiang, M., Xu, G., Yin, W., Yu, J., Zhang, Q., Zhao, C., 2023. The second monocular depth estimation challenge, in: *Proceedings of the IEEE/CVF Conference on Computer Vision and Pattern Recognition (CVPR) Workshops*, pp. 3064–3076.
- Su, L., Chen, Y., Song, H., Li, W., 2023. A survey of maritime vision datasets. *Multimedia Tools and Applications* 82, 28873–28893.
- Sutton, R.S., Barto, A.G., et al., 1998. *Reinforcement learning: An introduction*, volume 1. MIT press Cambridge.
- Tobin, J., Fong, R., Ray, A., Schneider, J., Zaremba, W., Abbeel, P., 2017. Domain randomization for transferring deep neural networks from simulation to the real world, in: 2017 IEEE/RSJ international conference on intelligent robots and systems (IROS), IEEE. pp. 23–30.
- Trinh, L., Mercelis, S., Anwar, A., 2024. A comprehensive review of datasets and deep learning techniques for vision in unmanned surface vehicles. arXiv preprint arXiv:2412.01461.
- VSTEP Simulation, 2025. Nautis simulator. <https://vstepsimulation.com/nautis-simulator/> (accessed 21 March 2025).
- Wärtsilä, 2025. Wärtsilä R&D simulator. <https://www.wartsila.com/marine/products/simulation-and-training/navigational-simulators/r-and-d-simulator> (accessed 21 March 2025).
- Yoon, H.K., Rhee, K.P., 2003. Identification of hydrodynamic coefficients in ship maneuvering equations of motion by estimation-before-modeling technique. *Ocean Engineering* 30, 2379–2404. URL: <https://www.sciencedirect.com/science/article/pii/S0029801803001069>, doi:[https://doi.org/10.1016/S0029-8018\(03\)00106-9](https://doi.org/10.1016/S0029-8018(03)00106-9).
- You, X., Yan, X., Liu, J., Li, S., Liu, Y., 2023. A novel model-based parameters estimation combining local optimization and global optimization of nonlinear ship models with physical experiment dataset. arXiv preprint arXiv:2312.05644.
- Zhang, A., Wang, W., Bi, W., Huang, Z., 2024. A path planning method based on deep reinforcement learning for auv in complex marine environment. *Ocean Engineering* 313, 119354.
- Zheng, H., Negenborn, R.R., Lodewijks, G., 2014. Trajectory tracking of autonomous vessels using model predictive control. *IFAC Proceedings Volumes* 47, 8812–8818.
- Zhou, L., Zhang, L., Konz, N., 2022. Computer vision techniques in manufacturing. *IEEE Transactions on Systems, Man, and Cybernetics: Systems* 53, 105–117.
- Žust, L., Kristan, M., 2022. Temporal context for robust maritime obstacle detection, in: 2022 IEEE/RSJ International Conference on Intelligent Robots and Systems (IROS), IEEE. pp. 6340–6346.